Electronic Supplementary Material (ESI) for Journal of Materials Chemistry C.

Supplementary Information

Ultrapure Deep-Blue Aggregation-Induced Emission and Thermally Activated Delayed Fluorescence Emitters for Efficient OLEDs with CIE_y < 0.1 and Low Efficiency Roll-Off

Jinshan Wang, *[a] Yuguang Yang, [a] Cuifeng Jiang, [a] Meng He, [a] Chuang Yao*[b] and Jianfeng Zhang *[c]

[a] School of Materials Science and Engineering, Yancheng Institute of Technology, Yancheng 224051, P. R. China

[b] Chongqing Key Laboratory of Extraordinary Bond Engineering and Advance Materials Technology (EBEAM), Yangtze Normal University, Chongqing 408100, P. R. China

[c] School of Physics and Optoelectronic Engineering, Guangdong University of Technology, Guangzhou 510006, P. R. China

1. General information

All reactants and solvents used for synthesis and other experiments were commercially available and used without further purification unless otherwise specified. ^{1}HNMR and ^{13}CNMR spectra were recorded on a Bruker AVANCE III HD 400 MHz spectrometer operating at 300 and 100 MHz, respectively, using tetramethylsilane (TMS) as the internal standard. Cyclic voltammetry (CV) was measured on a CHI-604E electro-chemical workstation with three-electrode system at a scan rate of 100 mV s^{-1}, in which glassy carbon electrode, Pt wire electrode and Ag/AgCl electrode as working electrode, counter electrode and reference electrode, respectively. A solution of tetra-*n*-butylammonium hexafluorophosphate (Bu_4NPF_6) (0.1 M) in dichloromethane (DCM) was used as electrolyte and the concentration of emitters was 1.0 × 10^{-3} M. Highest occupied molecular orbital (HOMO) energy level was determined from the onset potential of oxidation by cyclic voltammetry, E_{HOMO}=−(E_{onset}+4.4) eV; while lowest unoccupied molecular orbital (LUMO) energy level can be calculated using E_{HOMO} and optical band gap (E_g), E_{LUMO}=E_{HOMO}+E_g. Thermogravimetric analysis (TGA) and differential scanning calorimetry (DSC) measurements were conducted under nitrogen

atmosphere at a heating of rate 10 °C/min performed using a NETZSCH STA449F5 Jupiter Synchronous thermal analyzer. The glass transition temperatures are determined by the first heating cycle. Ultraviolet-visible (UV-vis) absorption and photoluminescence (PL) emission spectra were recorded with a Hitachi U-3900H spectrophotometer and Hitachi F-7000 fluorescence spectrometer, respectively. The PL lifetimes and absolute photoluminescent quantum yield of emitters in film were measured in an integrating sphere on an Edinburgh FLS920 fluoro-spectrophotometer. Single crystals of pCz-BTO was grown in the mixtures of dichloromethane/ methanol, and single crystal X-ray diffraction intensity data were collected at 293 K on Bruker Smart APEX II X-ray diffractometer equipped with a graphite-monochromated Cu-Kα radiation source (λ = 1.54184 Å). The structures were solved by a direct method and refined by full-matrix least squares on F^2 using the SHELX program.

2. Theoretical Calculation

The ground state geometries and electronic distributions of ICZ-DPS and ICZ-BP were optimized and calculated using the density function theory (DFT) method with B3LYP/6-31 G* basis set. The energy values of singlet and triplet were calculated by time-dependent DFT (TD-DFT) method at the same level.

3. Devices fabrication and characterization

ITO-coated glass (10 Ω sq^{-1}) substrates were pre-cleaned carefully before UV-ozone treatment for 6 min. The devices were prepared in vacuum at a pressure of 5×10^{-4} Pa. The organic layers were fabricated by thermally depositing at a rate of 1~2 Å/s. Subsequently, the deposition rate for LiF and Al were 0.1 Å/s and 3~5 Å/s, respectively. All the emitters were further purified by vacuum sublimation at temperature-gradient before OLEDs device fabrication by vacuum deposition. The current density-voltage characteristics, and luminance of the devices were measured by using a Keithley 2400 source meter and a calibrated silicon photodiode. The electroluminescence spectra

and luminance of the devices were measured on a PR650 spectrometer. Efficiencies of devices were calculated using EL spectra and current, assuming the devices were lambertian light sources.

4. Syntheses

*Synthesis of 3-(dibenzo[b,d]thiophen-4-yl)-9-phenyl-9H-carbazole (**BTC**):* **pCz-Br** (3.50g 11.0 mmol), **BT-BA** (2.28 g, 10.0 mmol), degassed toluene (30.0 mL) and degassed Na_2CO_3 (2 M aqueous solution, 10.0 mL) was added to a 100 mL schlenk flask. Then $Pd(PPh_3)_4$ (57.8mg, 0.50 mmol) was added to the solution and the mixture was stirred for 10 min under argon. The mixture was heated to reflux and kept for 72 hours. The reaction was then quenched with water (50.0 ml) and the mixture was extracted three times with chloroform (100.0 ml). The organic layer was dried with anhydrous sodium sulfate and the organic solvent was removed by rotary evaporation. The residue was purified by a short column chromatography with petroleum ether/dichloromethane as eluent yielding a white solid (3.70g, 86.9% yield), directly used for the next reaction.

*Synthesis of 4-(9-phenyl-9H-carbazol-3-yl)dibenzo[b,d]thiophene 5,5-dioxide (**pCz-BTO**):* ***BTC*** (3.0 g, 7.0 mmol) dissolve in 30 mL dichloromethane, then add 10.0 mL 30% hydrogen peroxide and 10.0 mL glacial acetic acid. The reaction was stopped after stirring for 24 hours under reflux. The reaction was then quenched with water (50.0 ml) and the mixture was extracted three times with chloroform (100.0 ml). The organic layer was dried with anhydrous sodium sulfate and the organic solvent was removed by rotary evaporation. The residue was purified by column chromatography using petroleum ether/**dichloromethane** as eluent to give ***pCz-BTO*** as a white solid (2.9g, 93.2% yield). ^{1}H NMR (300 MHz, $CDCl_3$): δ (ppm) 8.59 (d, *J* = 1.6 Hz, 1H), 8.23 (d, *J* = 7.7 Hz, 1H), 7.93 – 7.86 (m, 1H), 7.82 (dd, *J* = 12.4, 4.6 Hz, 3H), 7.71 (d, *J* = 7.6 Hz, 1H), 7.68 – 7.61 (m, 6H), 7.59 (d, *J* = 6.1 Hz, 1H), 7.54 (dd, *J* = 9.1, 5.5 Hz, 2H), 7.46 (d, *J* = 3.7 Hz, 2H), 7.37 – 7.30 (m, 1H). ^{13}C NMR (100 MHz, $CDCl_3$): δ (ppm) 141.55, 141.45, 141.20, 138.37, 137.63, 136.55, 135.76, 133.51, 133.42, 132.81, 132.60, 131.32, 131.13, 130.25, 129.89, 128.33, 127.62, 127.34, 127.21, 126.27, 123.69, 123.47, 123.31, 121.89, 121.53, 121.33, 120.64, 120.19, 119.59,

109.92, 109.79. Anal. Calcd for $C_{30}H_{19}NO_2S$: C, 78.75; H, 4.19; N, 3.06. Found: C, 78.53; H, 4.10; N, 2.99.

*Synthesis of 9-phenyl-3-(4-(phenylsulfonyl)phenyl)-9H-carbazole (**pCz-DPS**)*: **pCz-PBA** (1.2g, 3.25 mmol), **DPS-Br** (0.92g, 2.58 mmol), degassed toluene (30.0 mL) and degassed Na_2CO_3 (2 M aqueous solution, 10.0 mL) was added to a 100 mL schlenk flask. Then $Pd(PPh_3)_4$ (14.9mg, 0.13 mmol) was added to the solution and the mixture was stirred under argon bubbling for 10 min. The mixture was heated to reflux and reacted in argon atmosphere for 72 hours. Then the reaction was quenched with water (50 mL) and the mixture was extracted with chloroform (3 × 100 mL). The organic layer was dried over anhydrous sodium sulfate and the organic solvent was removed by rotary evaporation. The crude was purified by column chromatography using petroleum ether/**dichloromethane as the** as eluent to give ***pCz-DPS*** as a white solid (0.96 g, 80.7% yield). ^{1}H NMR (300 MHz, $CDCl_3$): δ (ppm) 8.38 – 8.34 (m, *J* = 1.5 Hz, 1H), 8.20 (d, *J* = 7.7 Hz, 1H), 8.08 (s, 1H), 8.05 (s, 2H), 8.02 (d, *J* = 1.8 Hz, 1H), 7.85 (d, *J* = 8.5 Hz, 2H), 7.71 – 7.65 (m, 2H), 7.63 (d, *J* = 1.7 Hz, 2H), 7.61 (d, *J* = 1.6 Hz, 2H), 7.58 (d, *J* = 1.8 Hz, 2H), 7.55 (s, 1H), 7.52 (d, *J* = 2.2 Hz, 1H), 7.50 (s, 1H), 7.47 (s, 1H), 7.45 (d, *J* = 1.2 Hz, 1H), 7.35 (m, *J* = 8.0, 6.0, 2.2 Hz, 1H). ^{13}C NMR (100 MHz, $CDCl_3$) δ 147.03, 142.12, 141.56, 141.11, 139.29, 137.42, 133.02, 131.18, 129.99, 129.26, 128.26, 127.87, 127.79, 127.62, 127.10, 126.51, 125.37, 124.09, 123.25, 120.39, 119.22, 110.34, 110.10. Anal. Calcd for $C_{30}H_{21}NO_2S$: C, 78.41; H, 4.61; N, 3.05. Found: C, 78.35; H, 4.53; N, 2.97.

*Synthesis of phenyl(4-(9-phenyl-9H-carbazol-3-yl)phenyl)methanone (**pCz-BP**)*: **pCz-PBA** (1.2g, 3.25 mmol), **BP-Br** (0.93g, 3.56 mmol), degassed toluene (30.0 mL) and degassed Na_2CO_3 (2 M aqueous solution, 10.0 mL) was added to a 100 mL schlenk flask. Then $Pd(PPh_3)_4$ (18.5 mg, 0.16 mmol) was added to the solution and the mixture was stirred under argon bubbling for 10 min. The mixture was heated to reflux and reacted in argon atmosphere for 72 hours. Then the reaction was quenched with water (50 mL) and the mixture was extracted with chloroform (3 × 100 mL). The organic layer was dried over anhydrous sodium sulfate and the organic solvent was removed by

rotary evaporation. The crude was purified by column chromatography using petroleum ether/**dichloromethane** as eluent to give **pCz-BP** as a white solid (1.10g, 80.3% yield). ^{1}H NMR (300 MHz, $CDCl_3$): δ (ppm) 8.46 (d, *J* = 1.3 Hz, 1H), 8.24 (d, *J* = 7.7 Hz, 1H), 7.98 (d, *J* = 8.4 Hz, 2H), 7.91 (s, 1H), 7.88 (s, 2H), 7.85 (s, 1H), 7.74 (dd, *J* = 8.6, 1.8 Hz, 1H), 7.67 (s, 1H), 7.63 (dd, *J* = 4.7, 2.7 Hz, 4H), 7.57 (s, 1H), 7.53 (dd, *J* = 4.4, 2.6 Hz, 3H), 7.51 (s, 1H), 7.49 – 7.45 (m, 2H), 7.36 (m, *J* = 8.0, 5.2, 3.0 Hz, 1H). ^{13}C NMR (100 MHz, $CDCl_3$): δ (ppm) 196.32, 146.13, 141.50, 140.93, 135.51, 132.25, 132.04, 130.88, 130.00, 128.30, 127.71, 127.11, 126.97, 126.39, 125.46, 124.06, 123.37, 120.42, 120.31, 119.12, 110.27, 110.06. Anal. Calcd for $C_{31}H_{21}NO$: C, 87.92; H, 5.00; N, 3.31. Found: C, 87.86; H, 4.91; N, 3.24.

5. Figures and Tables

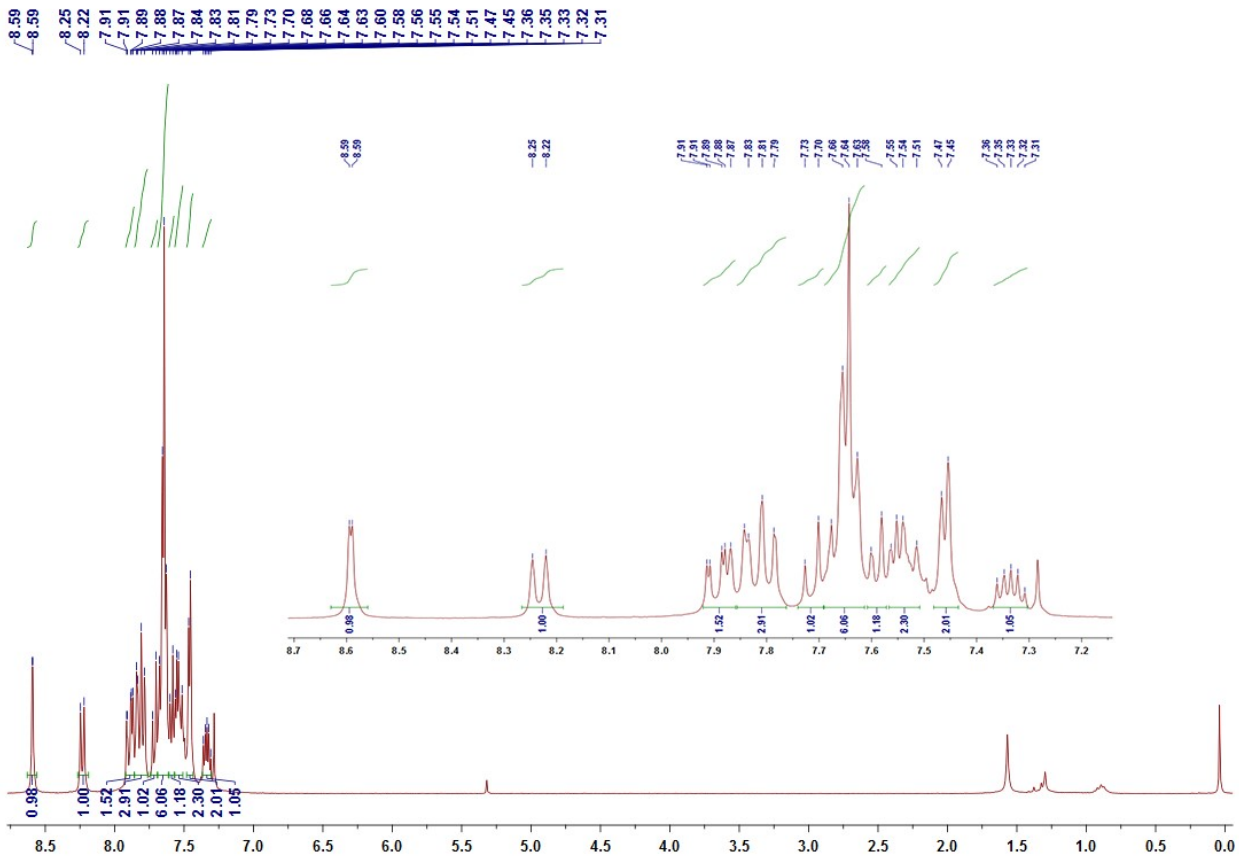

Fig. S1. ^{1}H NMR spectra of pCz-BTO

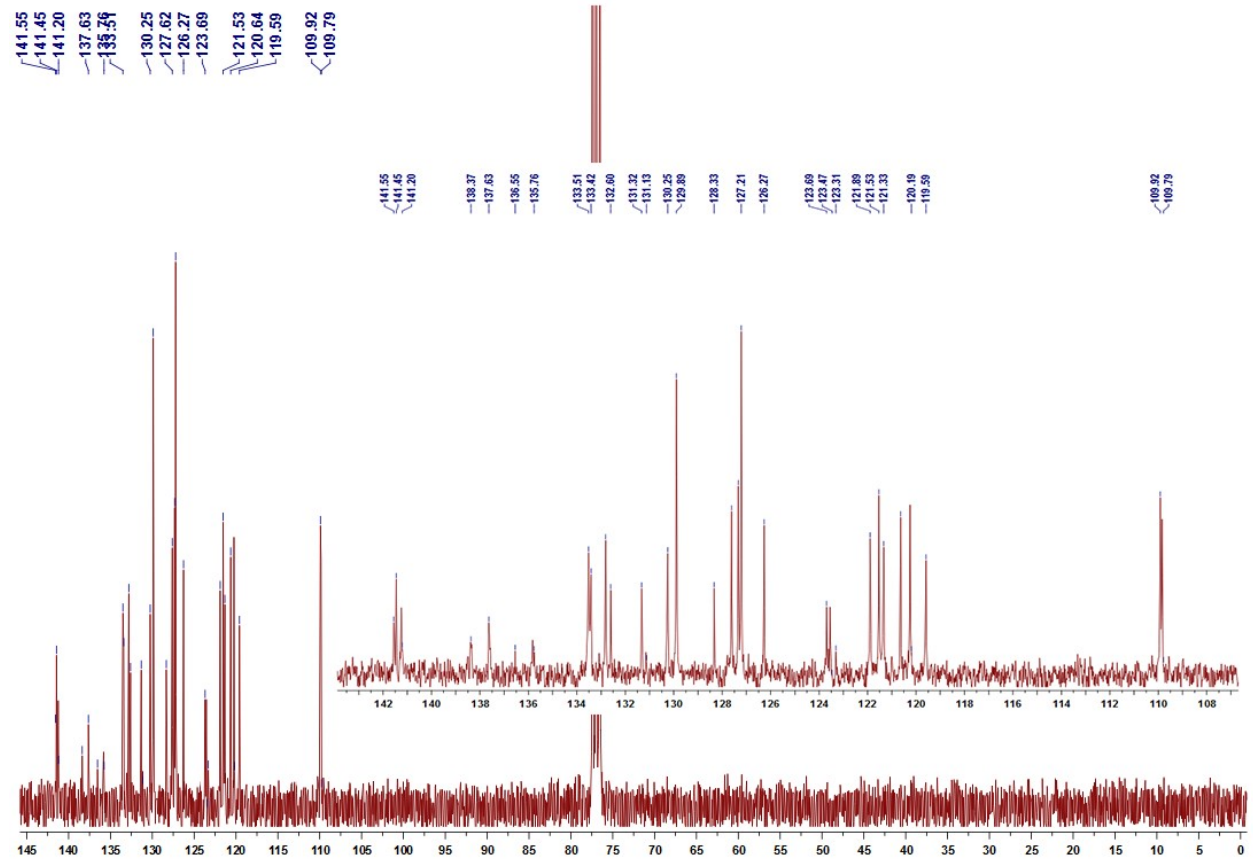

Fig. S2. ^{13}C NMR spectra of pCz-BTO

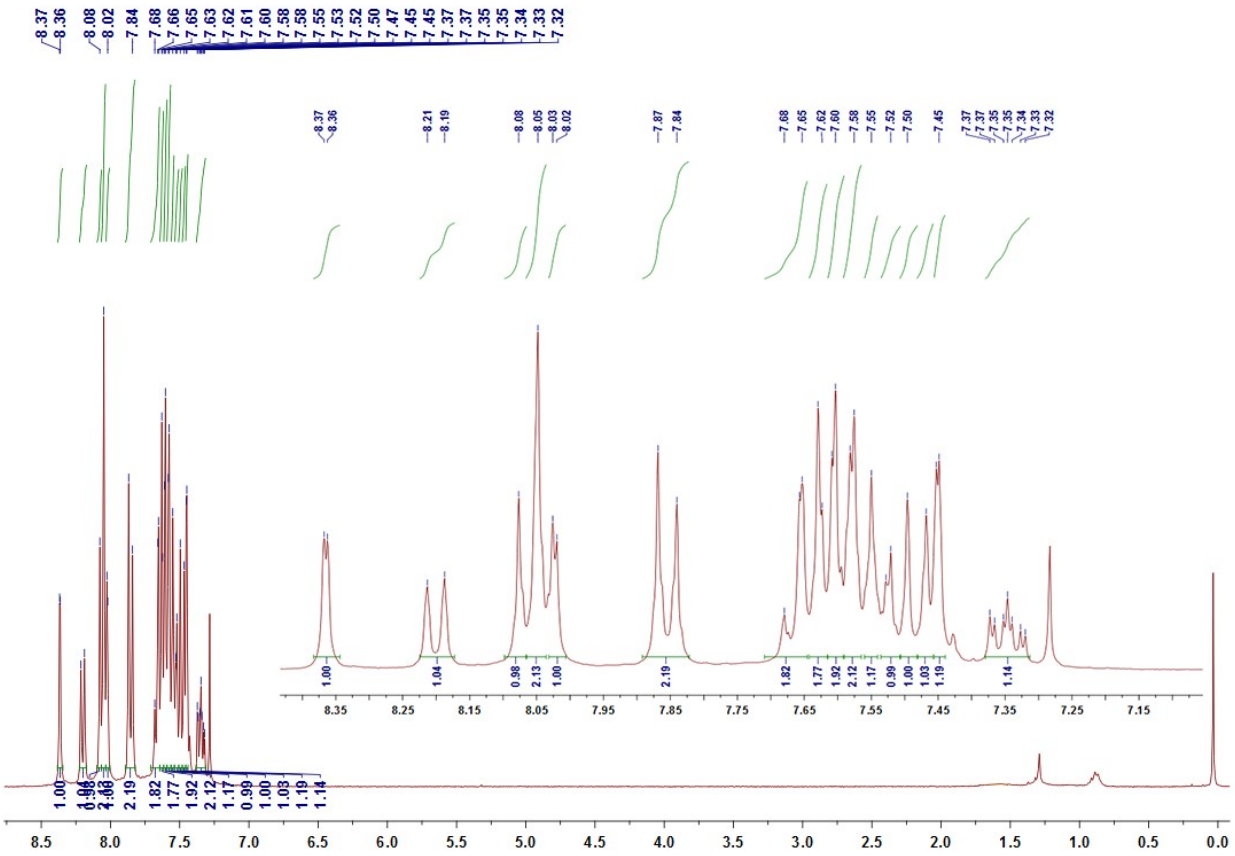

Fig. S3. ^{1}H NMR spectra of pCz-DPS

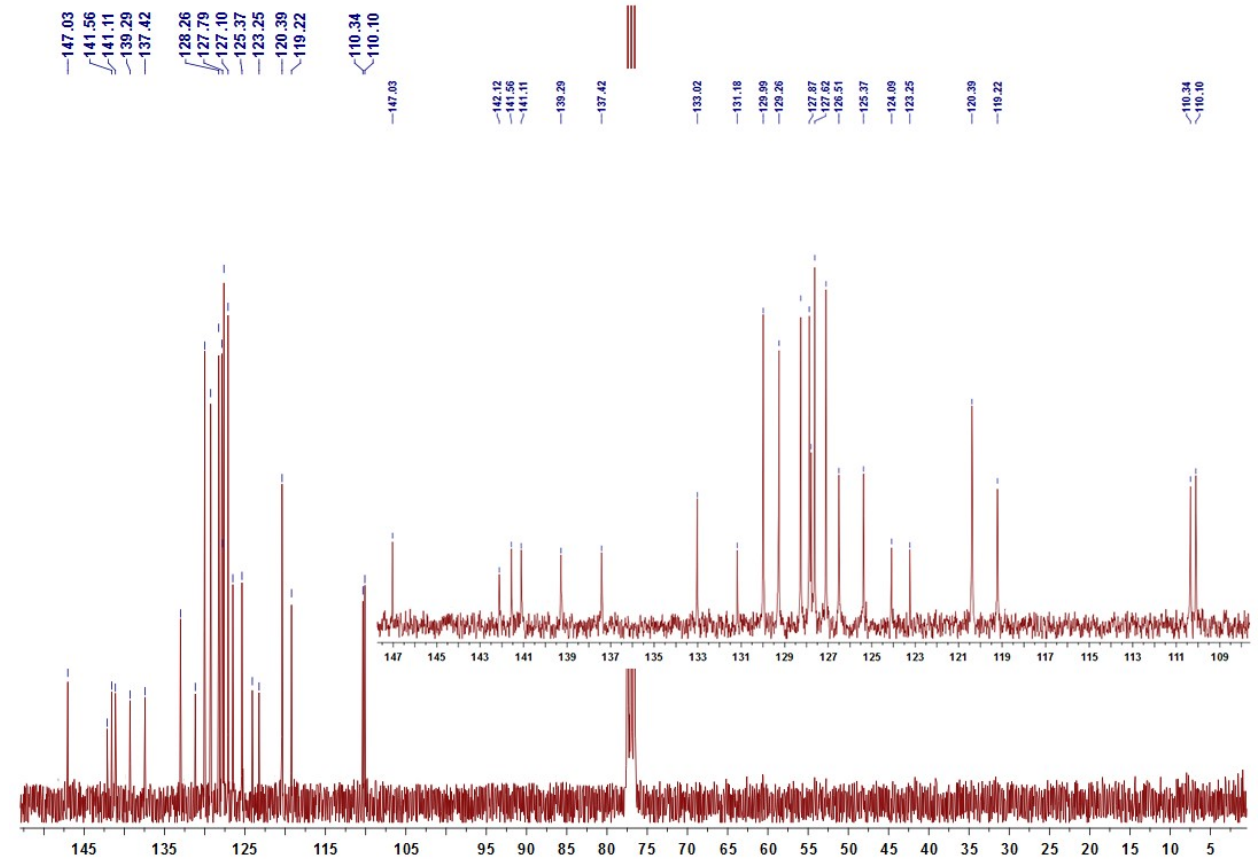

Fig. S4. ^{13}C NMR spectra of pCz-DPS

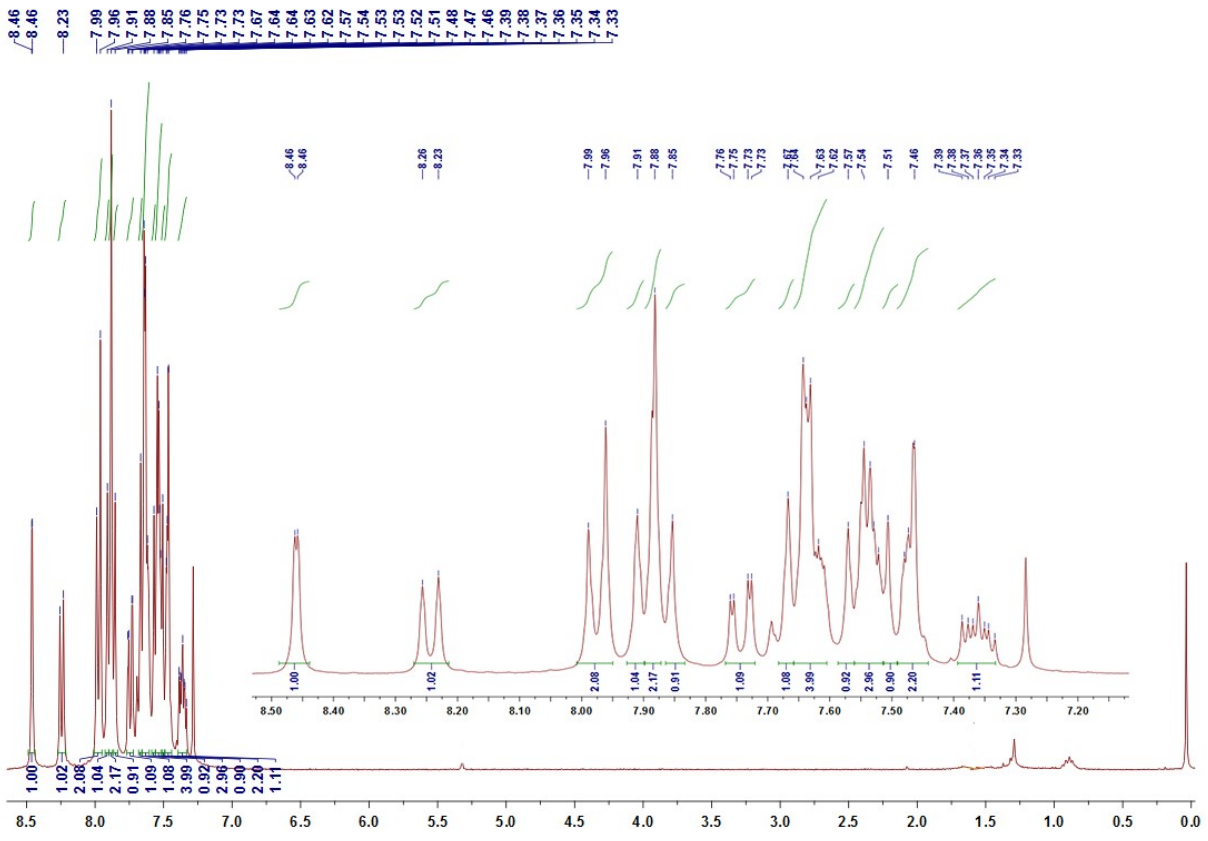

Fig. S5. ^{1}H NMR spectra of pCz-BP

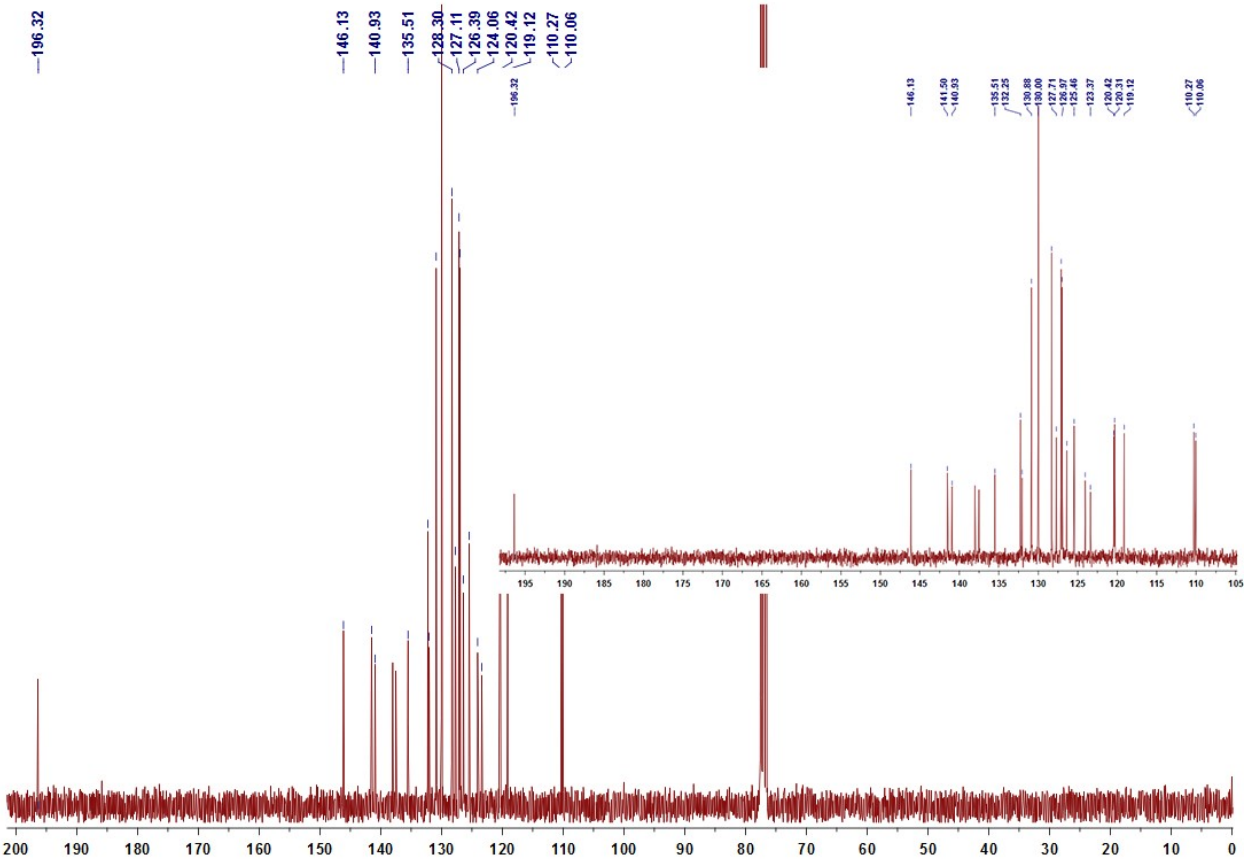

Fig. S6. ^{13}C NMR spectra of pCz-BP

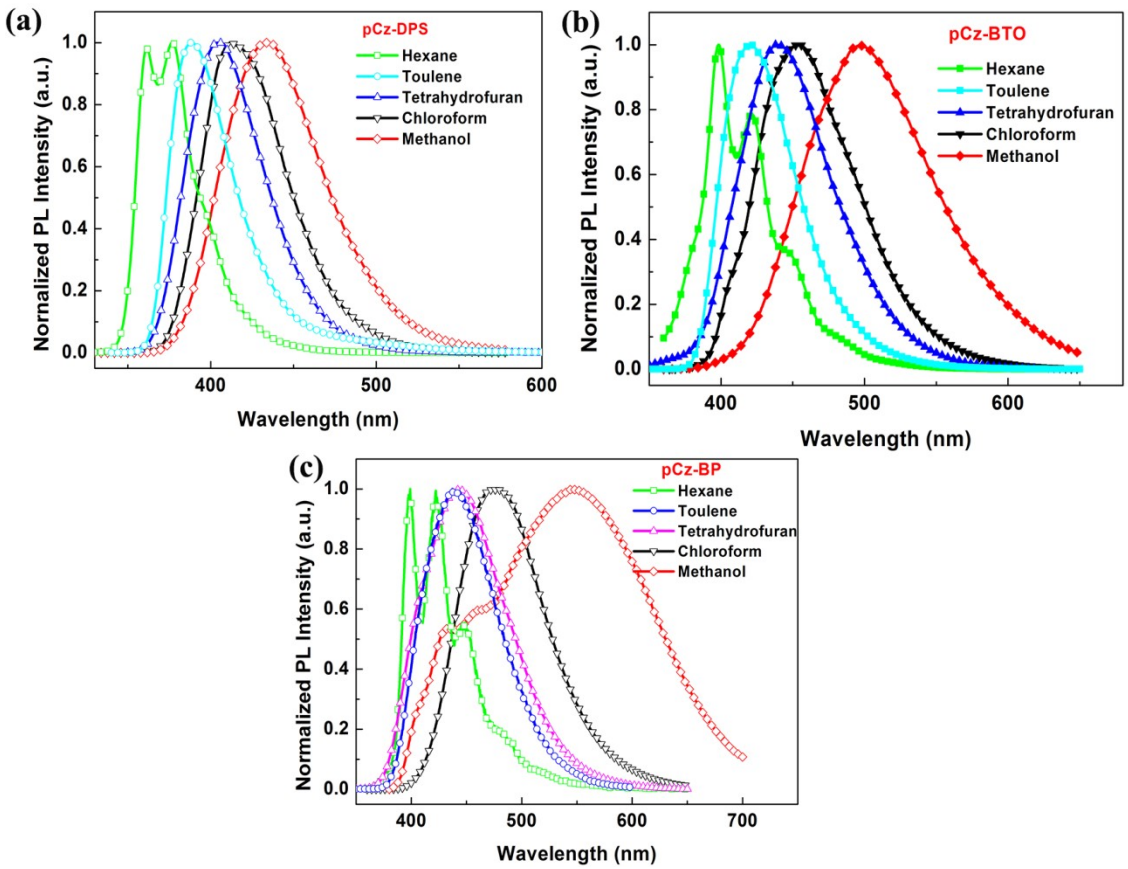

Fig. S7 The normalized PL spectra of pCz-DPS (a), pCz-BTO (b) and pCz-BP (c) in different solvent.

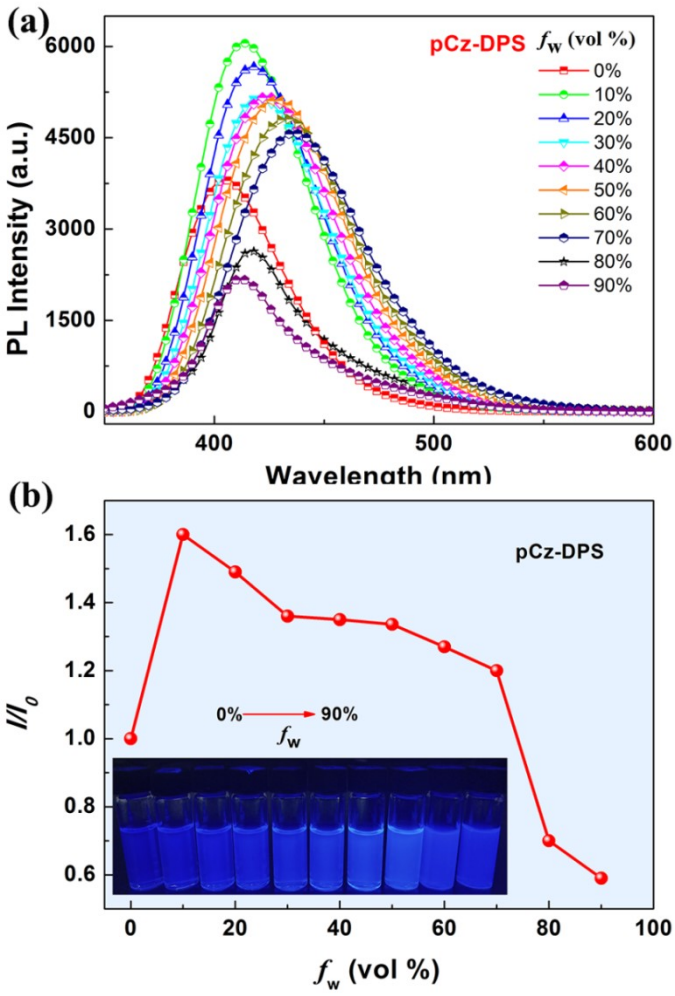

Fig. S8 (a) PL spectra in THF/water mixture with different water fraction (f_w) for pCz-DPS, solution concentration = 10 μM. (b) Plots of I/I_0 vs f_w (vol %) upon increasing the water content for PCZ-DPS. I_0 is the PL intensity in THF, and the inset pictures were taken under 365 nm excitation, representing luminogens in different THF/water mixtures (f_w = 0 to 90%).

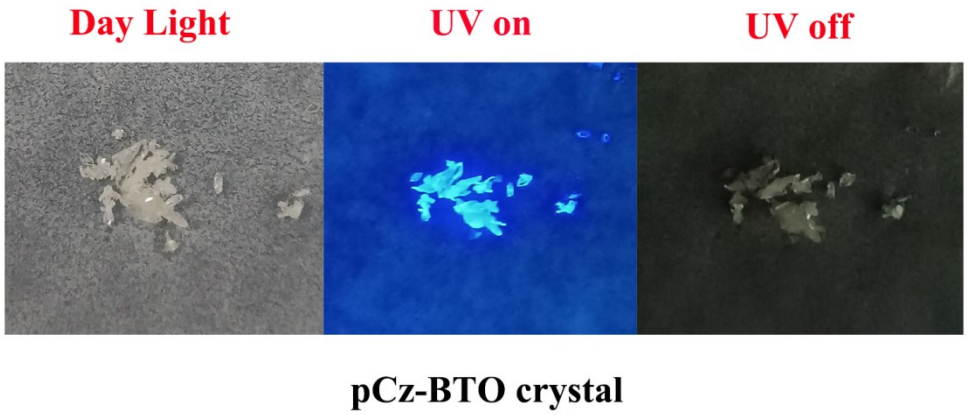

Fig. S9 Crystals picture of pCz-BTO in day light, under ultraviolet (UV) irradiation (365 nm) and after removal of UV.

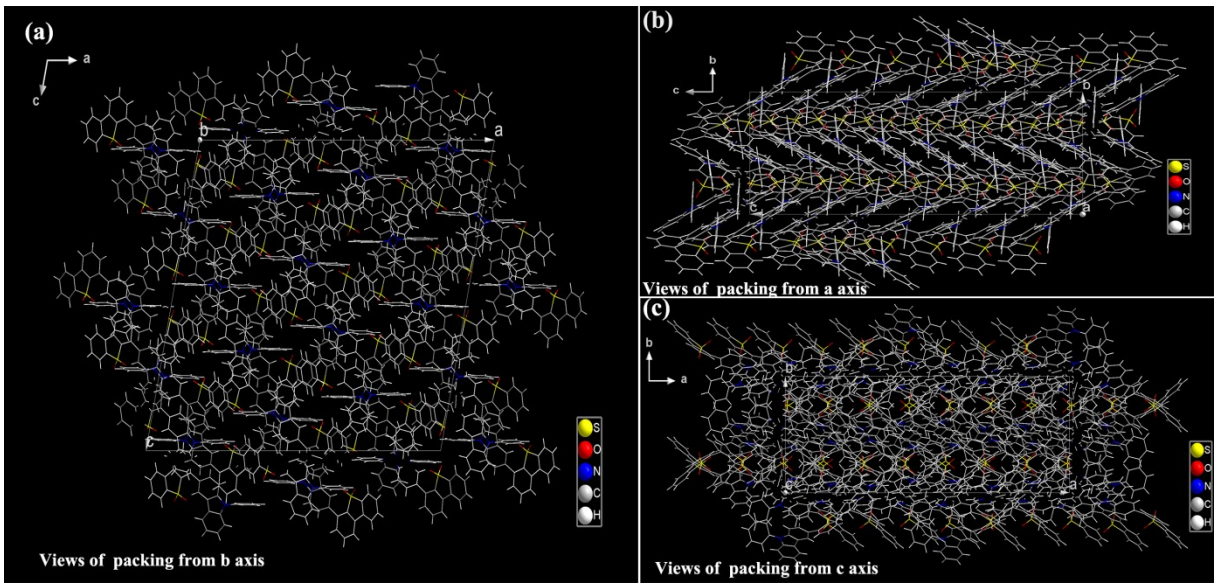

Fig. S10 Views of molecular packing of **pCz-BTO** from (a) *b* axis, (b) *a* axis and (c) *c* axis, respectively.

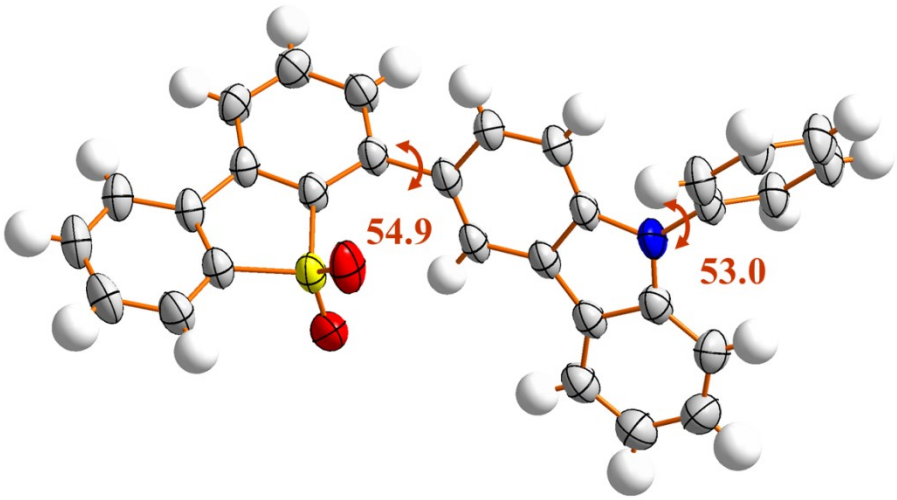

Fig. S11 Crystal structures of pCz-BTO with thermal ellipsoids set at 50% probability.

Table S1. Crystal data and structure refinement for pCz-BTO.

Identification code	pCz-BTO
Empirical formula	$C_{30}H_{19}NO_2S$
CCDC number	2094553
Formula weight	457.52
Temperature	293 K
Wavelength	1.54184 Å
Crystal system	Monoclinic
Space group	$P2_1/c$
Unit cell dimensions	a = 36.8845(4) Å α= 90°. b = 13.32330(10) Å β= 101.8620(10)°. c = 32.8389(3) Å γ = 90°.
Volume	15793.2(3) $Å^3$
Z	28
Density (calculated)	1.347 Mg/m^3
Absorption coefficient	1.500 mm^{-1}
F(000)	6664
Crystal size	0.15×0.08×0.06 mm^3
Theta range for data collection	2.448 to 68.357°
Index ranges	-44≤ h≤ 44, -14≤ k≤ 16, -39≤ l≤ 37
Reflections collected	165960
Independent reflections	28733 [R(int) = 0.0473]
Completeness to theta = 67.684°	99.90%
Absorption correction	Semi-empirical from equivalents
Max. and min. transmission	1.00000 and 0.30067
Refinement method	Full-matrix least-squares on F^2
Data / restraints / parameters	28733 / 0 / 2144
Goodness-of-fit on F^2	1.051
Final R indices [I>2sigma(I)]	R1 = 0.0508, wR2 = 0.1539
R indices (all data)	R1 = 0.0785, wR2 = 0.1774
Extinction coefficient	0.000086(8)
Largest diff. peak and hole	0.279 and -0.468 $e.Å^{-3}$

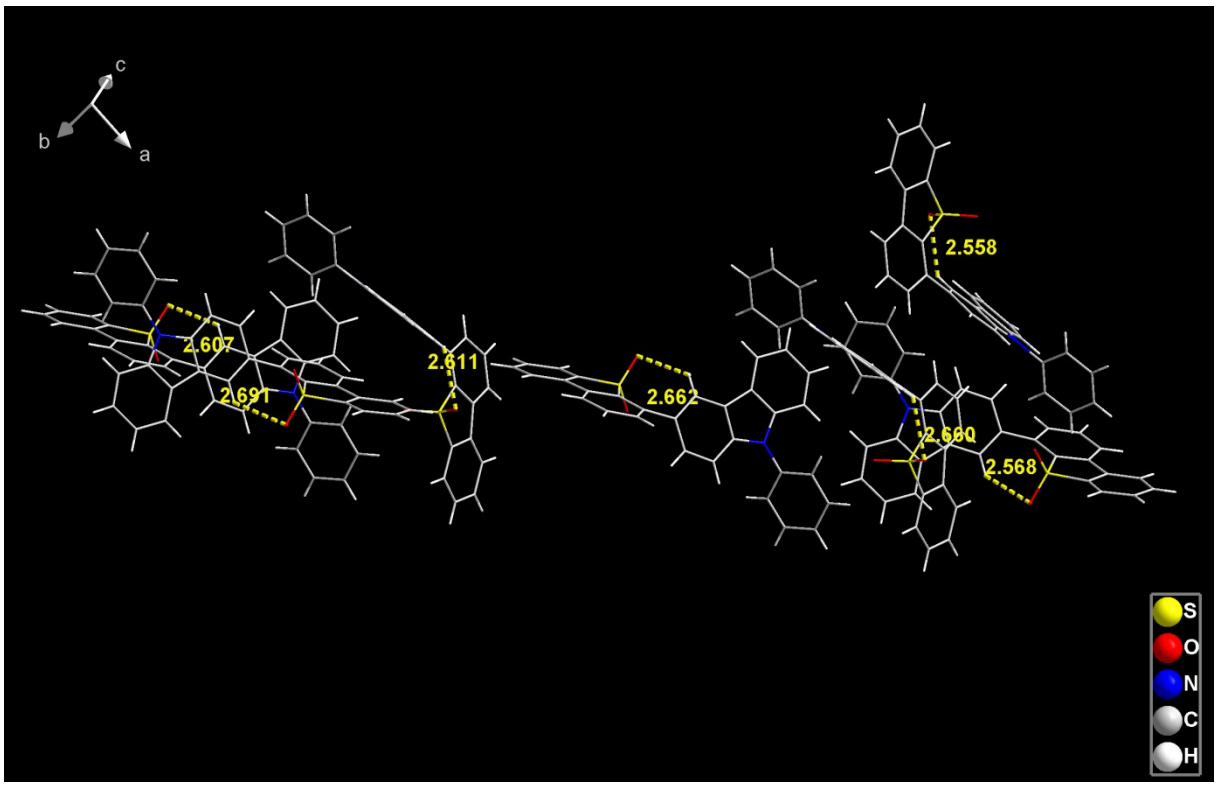

Fig. S12. The intramolecular C-H…O interactions in the crystals of pCz-BTO.

Table S2. Summarization of the interactions in the crystal of pCz-BTO. (intermolecular interactions: 1-22; intramolecular interactions: 23-29)

	Interactions	d /Å [a]	A /o [b]
1	C–H···O	2.563	154.378
2	C–H···O	2.565	123.259
3	C–H···O	2.914	109.945
4	C–H···O	3.222	109.408
5	C–H···O	2.585	123.23
6	C–H···O	2.603	122.835
7	C–H···O	2.558	123.034
8	C–H···O	2.585	122.121
9	C–H···O	3.166	158.789
10	C–H···π	3.289	157.072
11	C–H···π	2.971	132.452
12	C–H···π	3.612	139.813
13	C–H···π	3.334	160.350
14	C–H···π	3.640	157.969
15	C–H···π	3.015	150.461

16	C–H···π	2.923	160.663
17	C–H···π	3.170	145.427
18	C–H···π	3.230	146.948
19	C–H···N	3.185	107.561
20	C–H···N	3.209	112.208
21	C–H···N	2.933	123.938
22	C–H···N	2.988	126.006
23	C–H···O	2.607	125.487
24	C–H···O	2.691	123.548
25	C–H···O	2.611	130.435
26	C–H···O	2.662	122.825
27	C–H···O	2.558	129.808
28	C–H···O	2.660	127.139
29	C–H···O	2.568	131.547

[a] Distance of interactions. [b] Angel of C–H···O, C–H···N and C–H···π interactions.

Table S3. Summarized performances of OLEDs using and summary of reported deep blue TADF OLED devices with CIE y ≤ 0.1

Emission layer (neat films or host:emitter)	Peak [nm]	EQE_{max} (%)	EQE[a] @1000 cd/m^2	Roll-off[b] [%]	CIE	Ref.
TB-3Cz	424	9.90	−	−	(0.17, 0.07)	1
TB-P3Cz	448	6.13	−	−	(0.15, 0.08)	1
Py-2TP	448	3.46	−	−	(0.15, 0.09)	2
Py-2TF	444	2.10	−	−	(0.15, 0.08)	2
DPEPO:TDBA-SAF	456	28.2	17.6	37.5	(0.14, 0.09)	3
CzSi:PIAnCN		6.77	4.77	29.5	(0.15, 0.07)	4
CzSi:PA-TA	448	6.7	−	−	(0.15, 0.10)	5
PYD2:3b	435	8.50	−	−	(0.16, 0.08)	6
PPBI: PXB-mIC	450	12.5	5.2	58.4	(0.15, 0.08)	7
DCzBN2	417	7.7	−	−	(0.15, 0.07)	8
DCzBN3	414	10.3	−	−	(0.16, 0.06)	8
pCz-BTO	443	7.1	6.8 @3000 cd/m^2	4.2	(0.15, 0.10)	This work
DPEPO: pCz-BTO	443	9.5	9.0@3000 cd/m^2	5.3	(0.15, 0.09)	This work

a) External quantum efficiency at the luminance of 1000 cd m^{-2}. b) RO = EQE roll-off from peak value to that at 1000 cd m^{-2}.

6. References

[1] H. J. Kim, M. Godumala, S. K. Kim, J. Yoon, C. Y. Kim, H. Park, J. H. Kwon, M. J. Cho and D. H. Choi, *Adv*. *Opt*. *Mater*., 2020, **8**, 1902175.

[2] J. Yang, L. Li, Y. Yu. Z. Ren, Q. Peng, S. Ye, Q Li and Z. Li, *Mater*. *Chem*. *Front*., 2017, **1**, 91.

[3] H. Lim, H. J. Cheon, S. J. Woo, S. K. Kwon, Y. H. Kim and J. J. Kim, *Adv*. *Mater*., 2020, **32**, 2004083.

[4] X. Tang, Q. Bai, T. Shan, J. Li, Y. Gao, F. Liu, H. Liu, Q. Peng, B. Yang, F. Li and P. Lu, *Adv*. *Funct*. *Mater*., 2018, **28**, 1705813.

[5] Y. Wada, S. Kubo and H. Kaji, *Adv*. *Mater*., 2018, **30**, 1705641.

[6] N. Jurgensen, A. Kretzschmar, S. Hofle, J. Freudenberg, U. H. F. Bunz, *Chem*. *Mater*., 2017, **29**,

9154.

[7] D. H. Ahn, H. Lee, S. W. Kim, D. Karthik, J. Lee, H. Jeong, J. Y. Lee and J. H. Kwon, *ACS Appl*. *Mater*. *Interfaces*, 2019, **11**, 14909.

[8] C. Chan, L. Cui, J. U. Kim, H. Nakanotani and C. Adachi, *Adv*. *Funct*. *Mater*., 2018, **28**, 1706023.